

Constraints for high precision polarization detection at mm and sub-mm wavelengths from ground and space



Alessia Ritacco

*Laboratoire de Physique de l'École normale supérieure (LPENS)
Institut d'Astrophysique Spatiale (IAS) Paris*

Outline

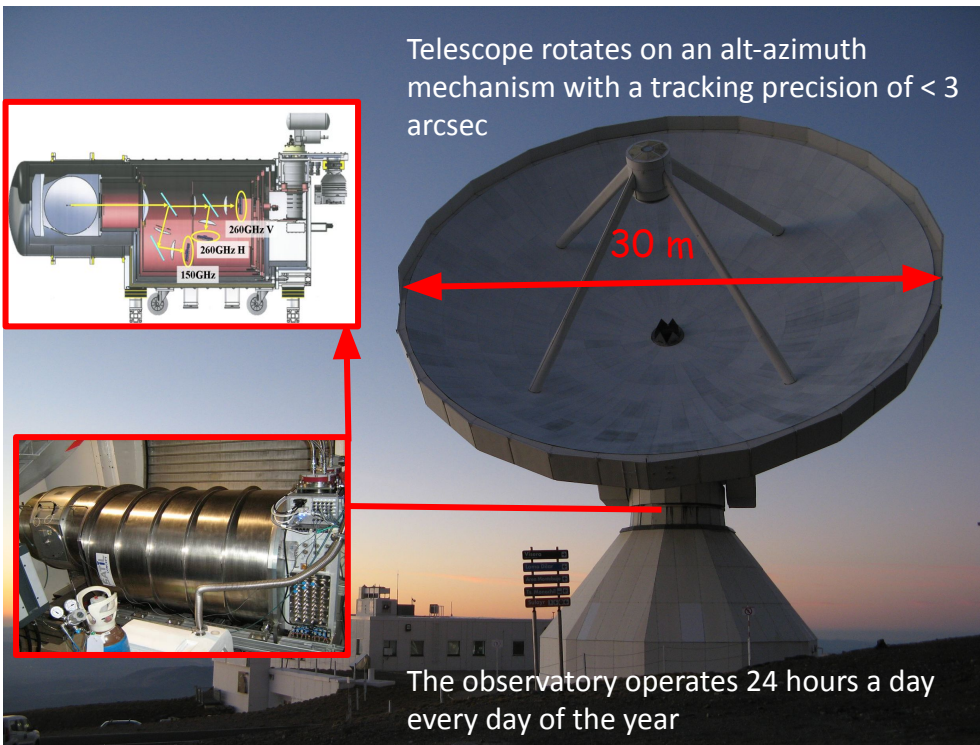
Technological development to unveil:

- Magnetic fields physics
NIKA2 from IRAM 30m telescope
- Cosmic Microwave Background polarization B-modes
CMB experiments - ex. LiteBIRD satellite

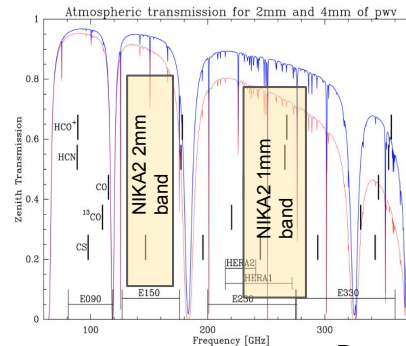
Polarization detection constraints:

- Mitigating systematics effects
- Absolute calibration
- Astrophysical foregrounds

NIKA2 at IRAM 30m telescope



NIKA2 continuum camera: 6.5 arcmin of FoV
2mm band: 125-170 GHz FWHM 17 arcsec
1mm band: 240-280 GHz FWHM 11 arcsec



Perotto et al. 2020

Science:

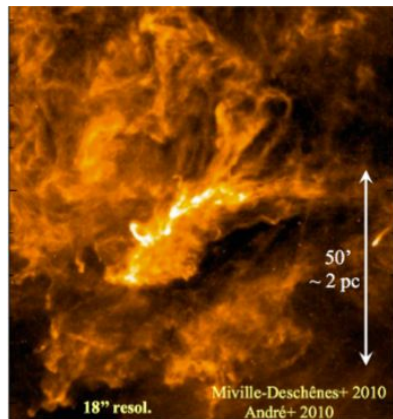
- Star formation;
- Galactic and extragalactic physics;
- Cosmology through the SZ effect in galaxy clusters;
- Solar system.

Motivations for NIKA2 polarimeter development: magnetic field structures in galactic regions

Herschel satellite results suggest a filamentary paradigm of star formation

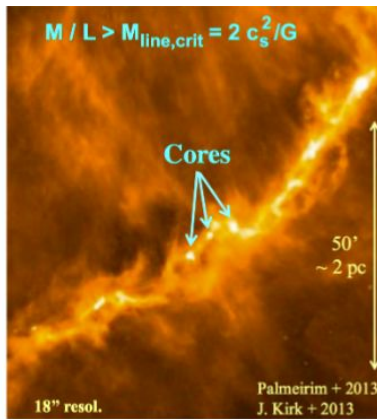
Planck polarization results reveal a well organized magnetic field at large angular scales

Large scale MHD turbulent flows generate filaments



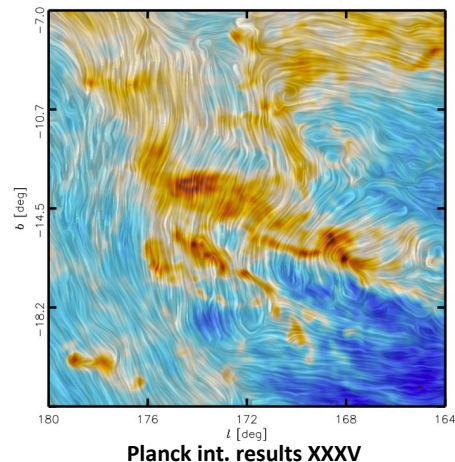
Polaris - Herschel/Spire 250 μm
Ref: *Protostars and Planets VI* review

Gravity fragments the densest filaments into prestellar cores

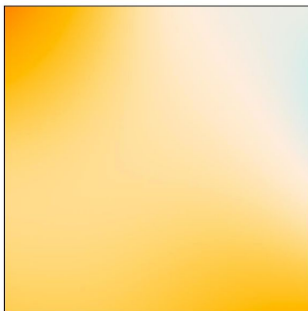


Taurus B211/3 - Herschel
André, Di Francesco, Ward-Thompson+2014

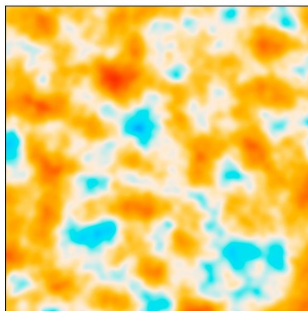
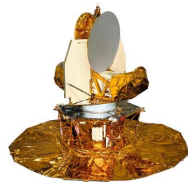
Taurus: columns density + B lines



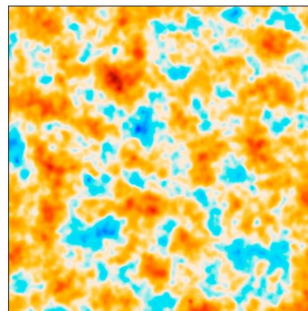
Need of high angular resolution observations to resolve the width of filaments $\sim 0.01\text{-}0.05$ pc



COBE

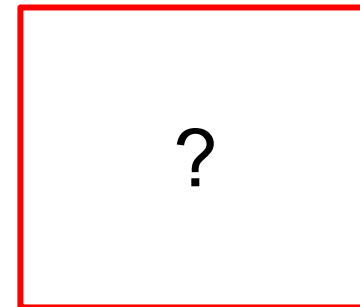


WMAP



Planck

What's next

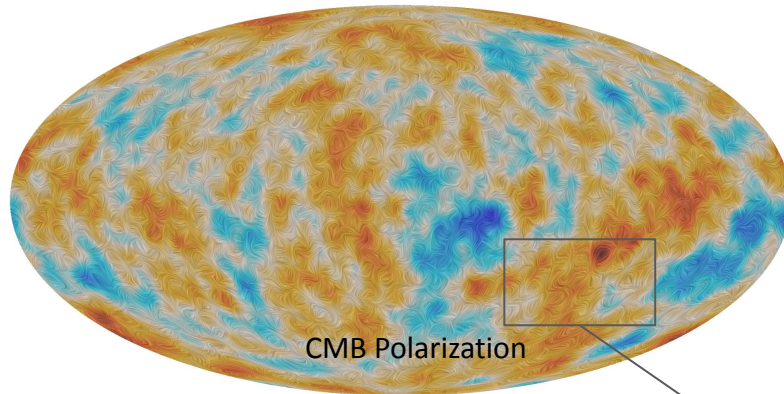
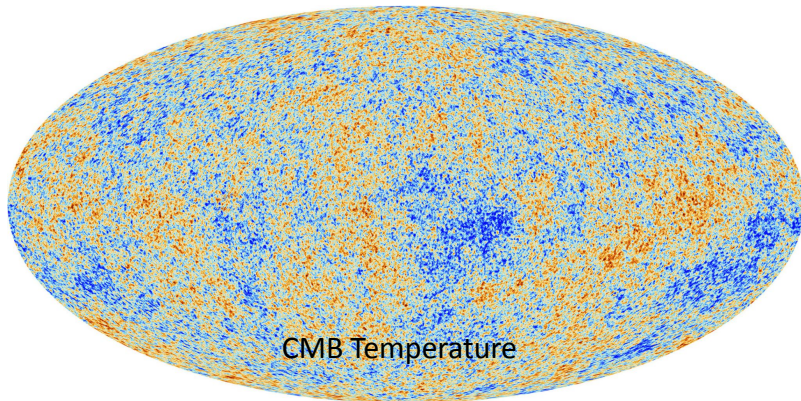


Technological challenges, systematics and calibration

Beyond Planck satellite observations

Planck satellite provided the best full-sky maps of Cosmic Microwave Background (CMB) to date in both temperature and polarization.

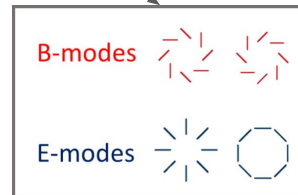
Credits: ESA and Planck collaboration



CMB polarization patterns can be expressed as the superposition of two different modes: the **E-modes**, of even parity, and the **B-modes**.

B-modes can only be produced by primordial gravitational waves in the early universe.

If detected they will probe the existence of an inflationary epoch and give us access to a physics beyond the current Standard Model.



Scientific motivations: CMB-B modes detection constraints

TT spectrum: cosmological parameters from density perturbations

EE spectrum: model coherence, break degeneracies

BB lensing spectrum: gravitational lensing of EE-modes, large-scale structures

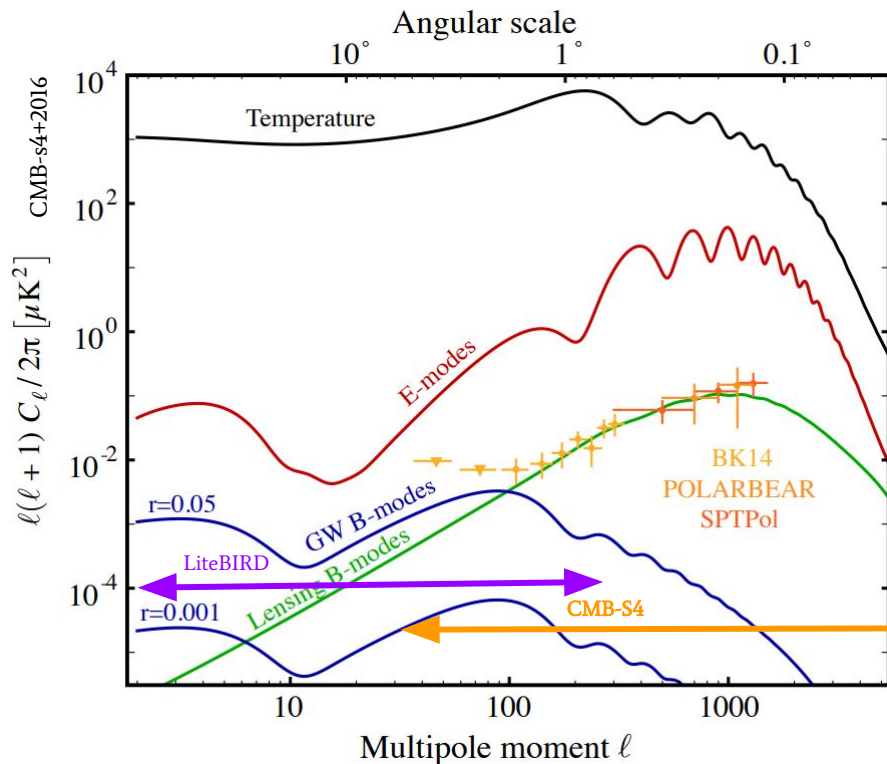
BB primordial spectrum: tensor perturbations from primordial GW background, scaled by tensor to scalar ratio r

Best upper limit is $r < 0.044$ [Planck low-l, BICEP2/Keck and Planck dust, Tristram + 2020]

Experiments under development are designed to target $\sigma(r) < 10^{-3}$

LiteBIRD $2 \leq \ell \leq 300$

CMB-S4 $30 \leq \ell \leq 5000$

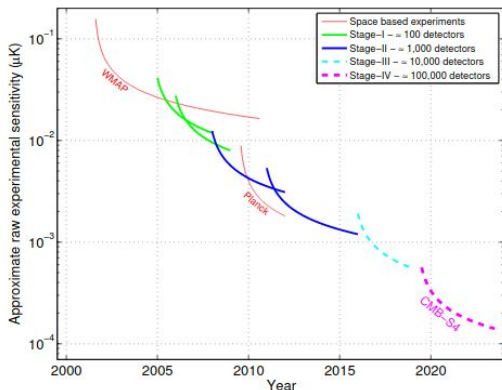


CMB experiments panorama

Noise challenge:

→ decreases increasing the number of detectors

GROUND



The next generation "Stage-4" ground-based CMB experiment.

Current Stage III

South Pole Telescope:

~ 16400 detectors

freq. 95-150-220 GHz

BICEP3:

2560 detectors @ 95GHz

Keck Array telescopes:

~29000 detectors

@ 35, 95, 150, 220, 270 GHz

Uncertainty expected on tensor-to-scalar ratio $r < 10^{-3}$

SPACE



LiteBIRD satellite conceptual design

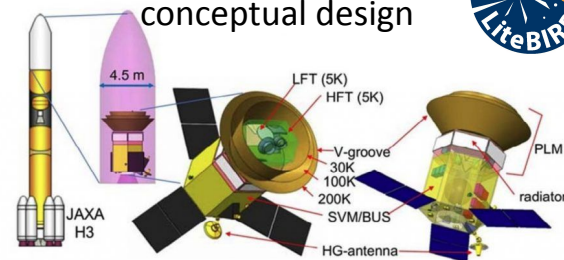


FIGURE 1-1 - OVERALL DESIGN OF THE LITEBIRD SPACECRAFT (courtesy JAXA)

Table 2. LiteBIRD telescope parameters

Telescope	Low freq.	Medium freq.	High freq.
Frequency	34–161 GHz	89–224 GHz	166–448 GHz
Telescope field of view	20° × 10°	28° diameter	28° diameter
Aperture diameter	400 mm	300 mm	200 mm
Angular resolution	70–24 arcmin	38–28 arcmin	29–18 arcmin
Rotational HWP	46–83 rpm	39–70 rpm	61–110 rpm
Number of detectors	1248	2074	1354

High precision polarization detection challenges

Instrumental improvements:

Increasing SNR and reducing instrumental noise

- Arrays of high sensitive detectors
- **Half wave plates:**
from ground it also dramatically reduces correlated atmospheric noise.

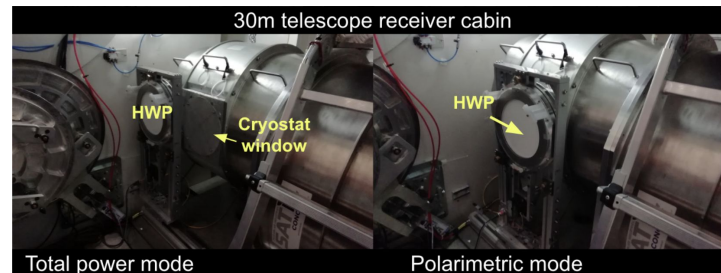
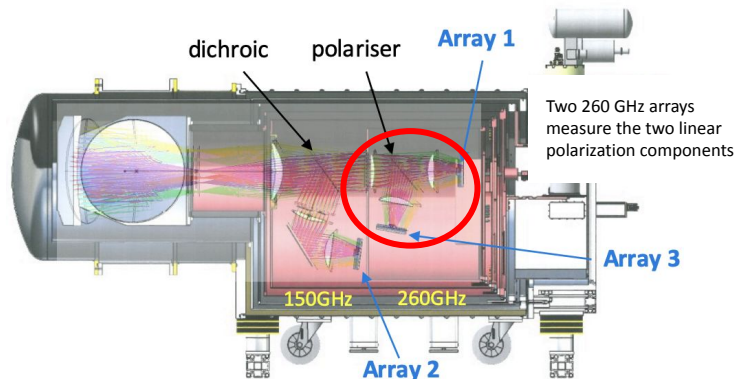
Calibration: high control of systematics, absolute accuracy of the polarization reconstruction.

Astrophysical foregrounds:

Component separation → large frequency range coverage

NIKA2 polarimeter

Half wave plate modulator



Modulating the polarization signal with a rotating half wave plate has numerous advantages:

- It separates the polarization signal from the unpolarized one
- A single polarized detector measures simultaneously the polarization parameters Stokes Q and U
- The signal is shifted far from 1/f noise
- It mitigates several systematics (atmosphere, thermal drifts, beam mismatch, asymmetries...)
- But it can introduce new systematic effects (Ritacco+17, D'Alessandro+2019) that need to be carefully addressed

Data model

$$\begin{aligned}
 d_k(t)(f_b, t) = & \frac{1}{2} \mathbf{A}_{t,p} \{ I_p + \rho_{\text{pol}} [Q_p \cos(4\omega t + 2\psi_k(t)) + U_p \sin(4\omega t + 2\psi_k(t))] \} \times \alpha_k \times \gamma^{\text{atm}}(\tau^{\text{atm}}) \\
 & + \text{HW}PSS(\omega) + \alpha_k^{\text{atm}} A_k(f_b, t) + n_k(t) \\
 & + G_k(t) + \epsilon_k(t) E_k(f_b, t) + C_k(t) + \mathcal{I}\mathcal{P}
 \end{aligned}$$

Control of Half Wave Plate systematics

Data model

$$d_k(t)(f_b, t) = \frac{1}{2} \mathbf{A}_{t,p} \{ I_p + \text{Incoming polarization modulated at 4 times the HWP rotation frequency} \} \times \text{Atmospheric absorption}$$

$$+ \text{HWP Synchronous Signal} + \text{Atmospheric emission} + \text{Detector noise}$$

$$+ \text{Glitches terms} + \text{Electronic noise} + \text{Cryogenic noise} + \text{Instrumental polarization}$$

Ritacco et al. A&A 599, A34 (2017)

Instrumental polarization:

Linear polarization from unpolarized sky emission

HWP cross-polarization → Leakage of polarisation from one axis to the other

Drifts of the HWP temperature with time → Different emissivities

Deterioration of the beam passing through the HWP (ellipticity)

Reflections at non-normal incidence can be detected at $4f (I > Q / U) \dots$

Mitigating the systematic effects

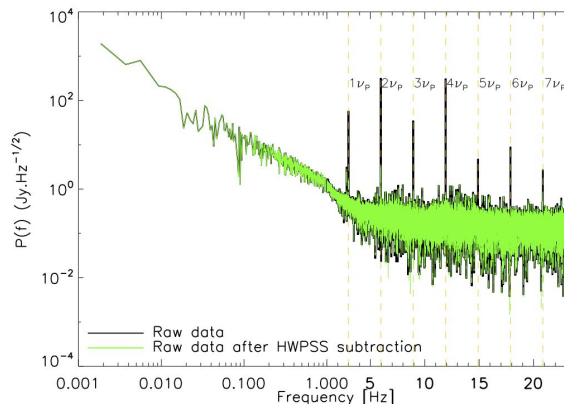
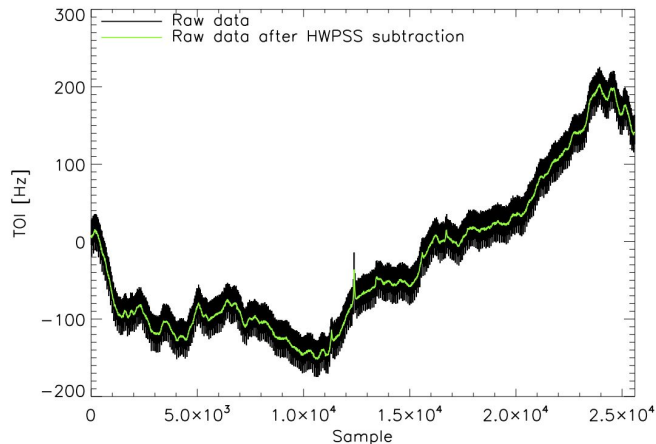
- * Absolute flux calibration instabilities due to atmospheric fluctuations
- * Polarization efficiency
- * Level of instrumental polarization \rightarrow I to P leakage
- * Absolute angle calibration
- * Side lobes ...

Mitigating the systematic effects

- * Absolute flux calibration instabilities due to atmospheric fluctuations
- * **Polarization efficiency**
- * Level of instrumental polarization → I to P leakage Ritacco et al. A&A 599, A34 (2017)
- * Absolute angle calibration
- * Side lobes ...

NIKA-example: continuous rotating multi-layers HWP produced a modulation also of the background signal

This HWP synchronous signal (HWPS) is peaked at harmonics of the HWP rotation frequency ν
Ritacco et al. 2017 modeled the HWPS (and subtracted it per TOI)

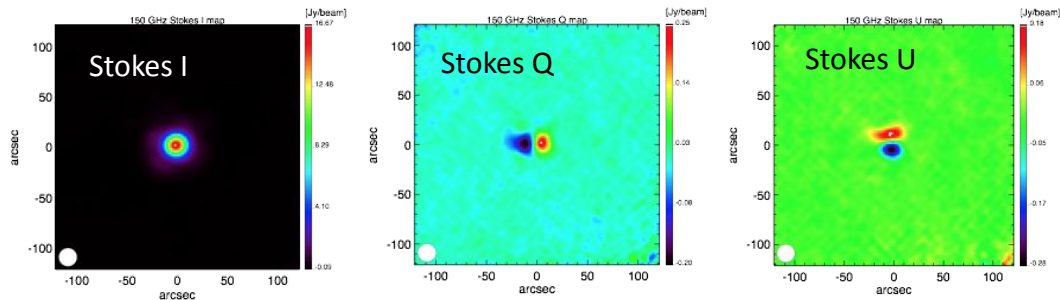


Mitigating the systematic effects

- * Absolute flux calibration instabilities due to atmospheric fluctuations
- * Polarization efficiency
- * **Level of instrumental polarization** → I to P leakage
- * Absolute angle calibration
- * Side lobes ...

NIKA/IRAM 30m case addressed in
 Ritacco et al. *A&A* 599, A34 (2017)

Unpolarized source: we expect **NO signal** in Stokes Q and U maps



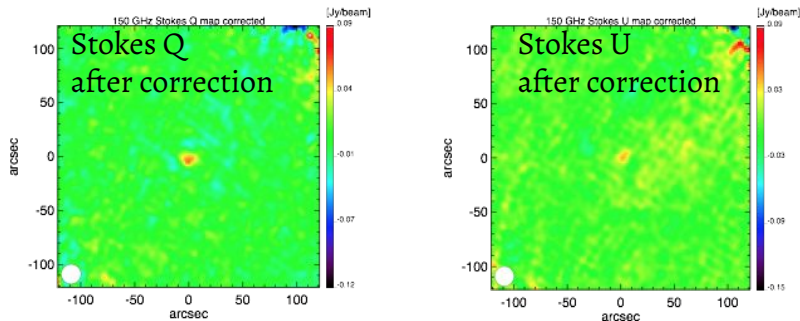
It depends on the optical elements including the HWP + detectors

Mitigating the systematic effects

- * Absolute flux calibration instabilities due to atmospheric fluctuations
- * Polarization efficiency
- * **Level of instrumental polarization** → I to P leakage
- * Absolute angle calibration
- * Side lobes ...

NIKA/IRAM 30m case addressed in
Ritacco et al. *A&A* 599, A34 (2017)

It can be modelled and subtracted if it is stable and common to all the detectors



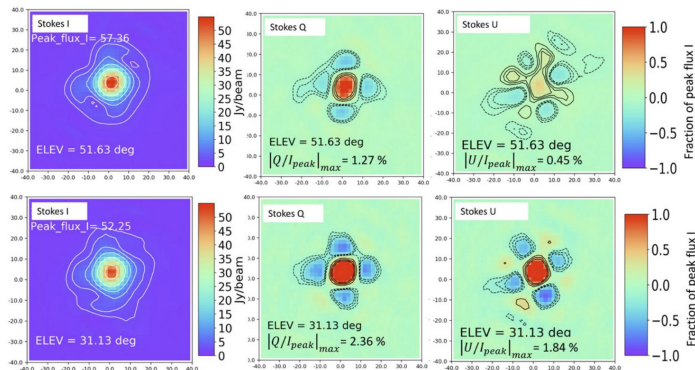
IP residual: 0.6 % of total intensity
→ to be accounted in the overall polarization
uncertainties budget

Mitigating the systematic effects

- * Absolute flux calibration instabilities due to atmospheric fluctuations
- * Polarization efficiency
- * **Level of instrumental polarization** → I to P leakage
- * Absolute angle calibration
- * Side lobes ...

NIKA2/IRAM 30m case preliminary investigation discussed in
Ajeddig et al. EPJ Web of Conferences 228, 00002 (2020)

NIKA2 has presented a more complicated pattern, which depends on many parameters



- Leakage effect not stable → difficult to be modelled
- A dependency with source elevation and focus has been observed and now we are close to model it and subtract it to all data sets

Mitigating the systematic effects

- * Absolute flux calibration instabilities due to atmospheric fluctuations
- * Polarization efficiency
- * Level of instrumental polarization → I to P leakage
- * **Absolute angle calibration**
- * Side lobes ...

Challenge for CMB-B modes detection constraints

A miscalibration of the absolute polarization angle by $\Delta\psi_{Gal}$ will lead to a mixing of E and B modes. In the CMB and because $C_l^{EE} \gg C_l^{BB}$, this is often referred to as an “E to B leakage” and reads

$$\tilde{C}_l^{BB} = C_l^{BB} \cos^2 2\Delta\psi_{Gal} + C_l^{EE} \sin^2 2\Delta\psi_{Gal}$$

$$\Leftrightarrow \Delta C_l^{BB} \simeq (2\Delta\psi_{Gal})^2 C_l^{EE}$$

Spurious bias component

Accuracy in the calibration of the polarization angle:

- Ground calibration: very good but **need to be validated during operations**
- External calibration source: good accuracy but **never done before, instrumental limits ?!**
- Self-calibration: we expect no scientific signal from TB and EB → only instrumental
→ **Losing constraints on fundamental phenomena**
- Sky calibration: **frequency dependence, time variability** → **Best option: CRAB NEBULA**

Accuracy of the polarization detection

A sky calibrator: the Crab nebula

* Absolute angle calibration

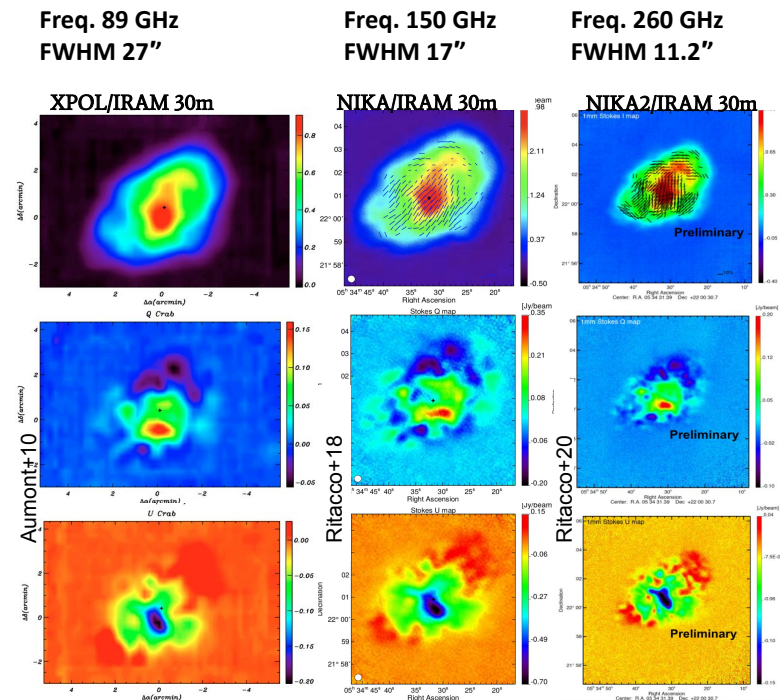
The **Crab Nebula** (Tau A) is a plerion-type supernova remnant, observed from radio to X-rays

The microwave emission has an extension of about $5' \times 7'$

Most intense polarized source in the microwave sky, at angular scales of few arcminutes

Highly polarized synchrotron emission with a polarization fraction of $\sim 20\%$

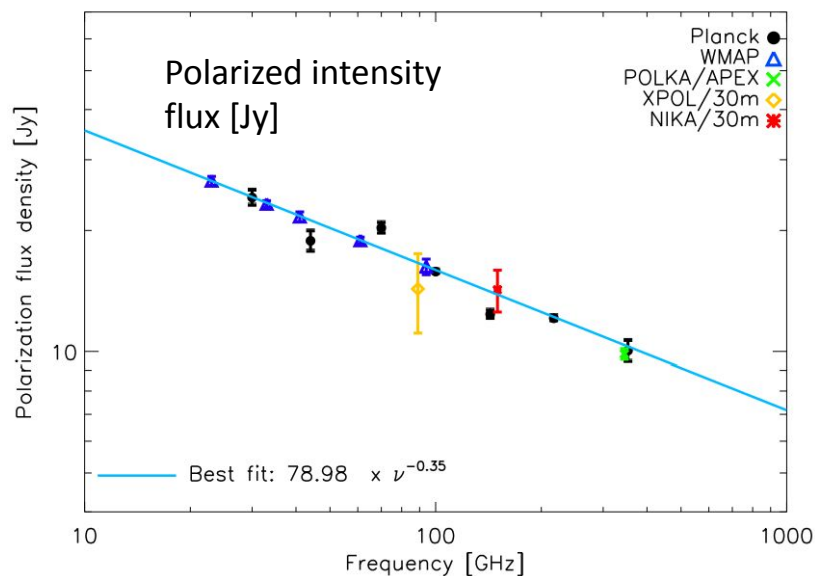
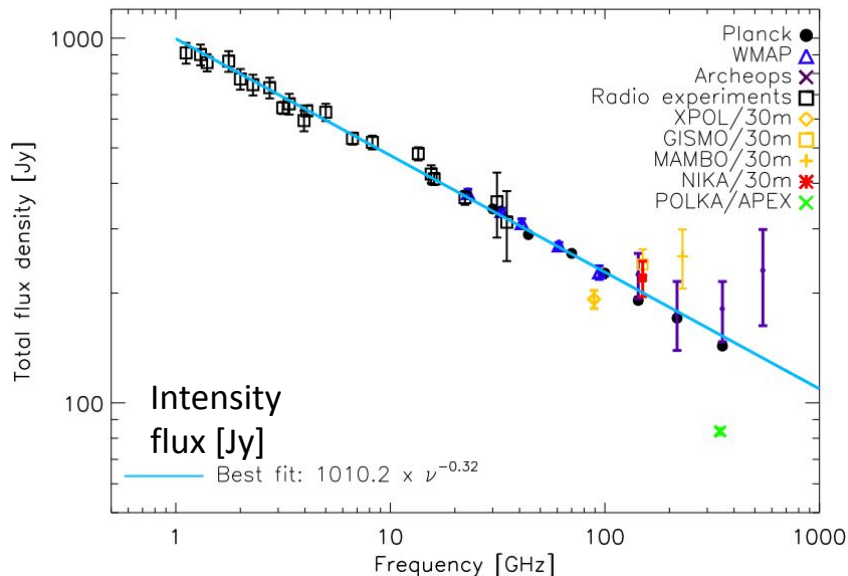
It is relatively isolated in the microwave sky within 1 degree scale



Spectral energy distribution (SED)

The **polarization spectral index** is consistent with the total power index confirming that the **synchrotron radiation from a single population of relativistic electrons** is responsible for the emission of the nebula.

$$\beta = -0.323 \pm 0.001 ; \beta_{POL} = -0.347 \pm 0.026.$$



*Planck HFI fluxes have been recomputed here by using aperture photometry techniques

Ritacco et al. 2018, A&A, 616, A35

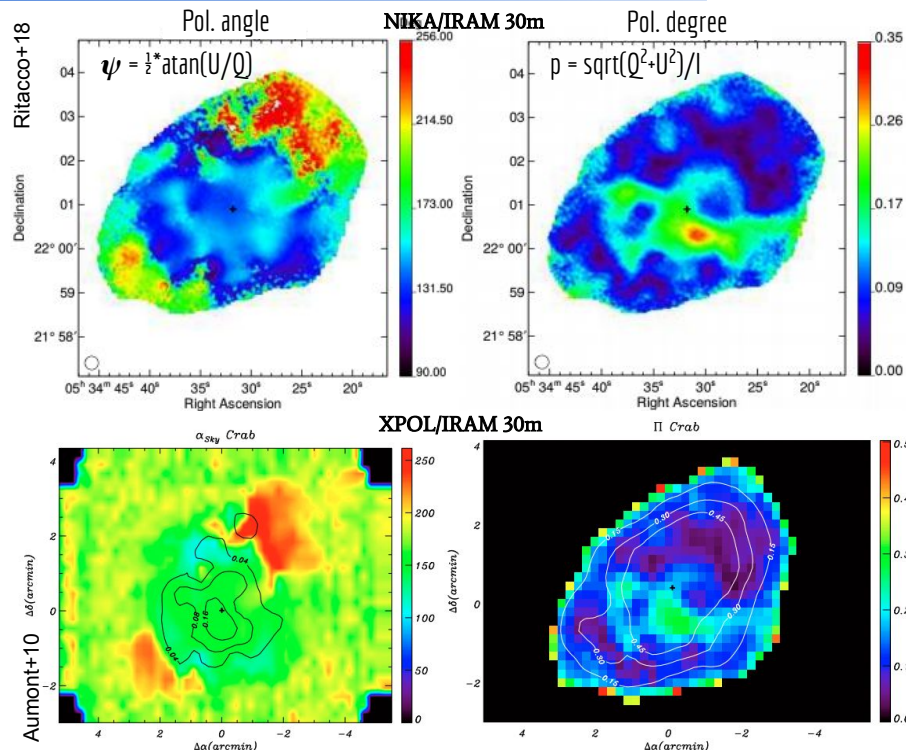
Ground based high angular resolution observations



A variation from small to large angular scales is observed on both the polarization angle and degree

The polarization direction appears stable with the frequency and constant within a radius of 2 arcmin from the Nebula center

In order to compare with CMB experiments results let's check the integrated flux across the source



Constraints of the absolute calibration

* Compilation of:

WMAP [Weiland+11]

Planck-LFI [Planck 2015 XXVI],

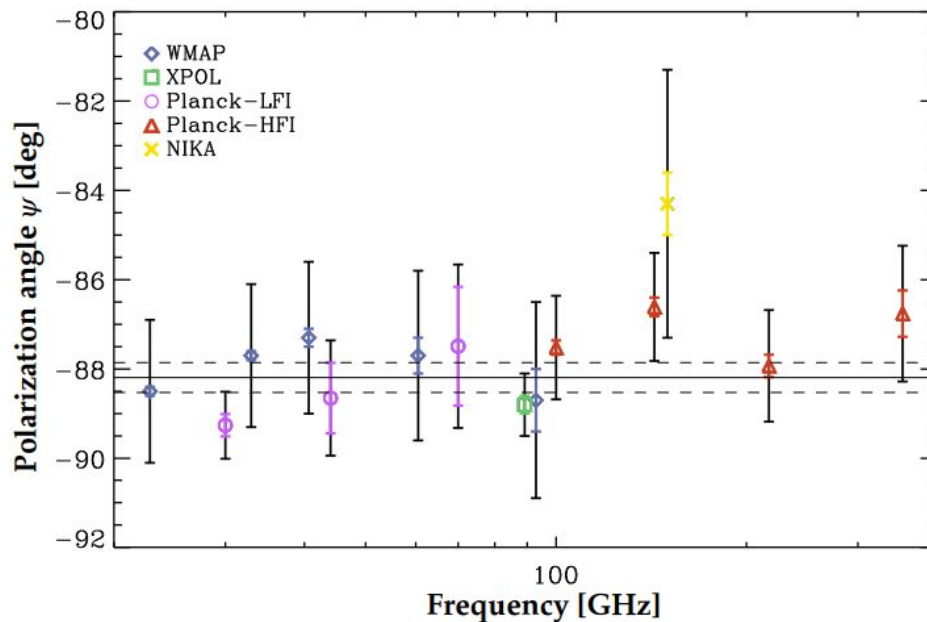
Planck-HFI, re-analyzed in [Ritacco+18])

XPOL\IRAM-30m [Aumont+10]

and NIKA\IRAM-30m [Ritacco+18]

Total weighted polarization angle average:

$$\psi = -88.26^\circ \pm 0.27^\circ$$



J. Aumont , J.F. Macías-Pérez, **A. Ritacco**, N. Ponthieu,
A. Mangilli A&A 634, A100 (2020)

Combining current (and future) measurements

Power spectrum bias from E-B mixing due to the miscalibration of the absolute polarization angle

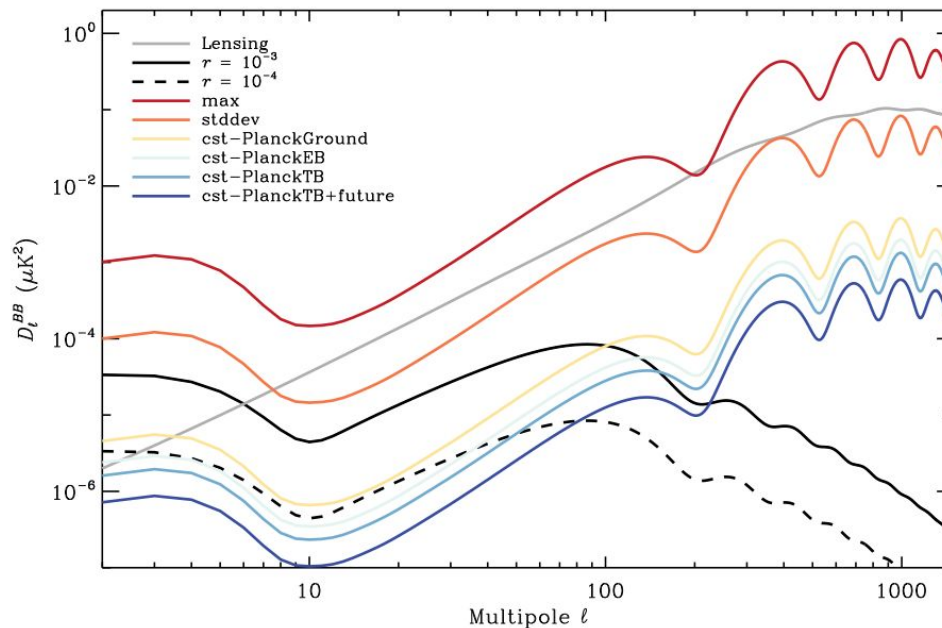
Aumont+2020

* Assumption of constant polarization angle is necessary to lower the D_l^{BB} bias

* Under the crucial assumption that the polarization angle is constant with frequency, the combined error $\sigma(\psi) \sim 0.27^\circ$ could allow to probe $r = 10^{-2}$

* Future accurate measurements of the Crab are needed to meet the requirements of future CMB experiments ($\sigma(\psi) \sim 0.1^\circ$) to measure $r = 10^{-3}$

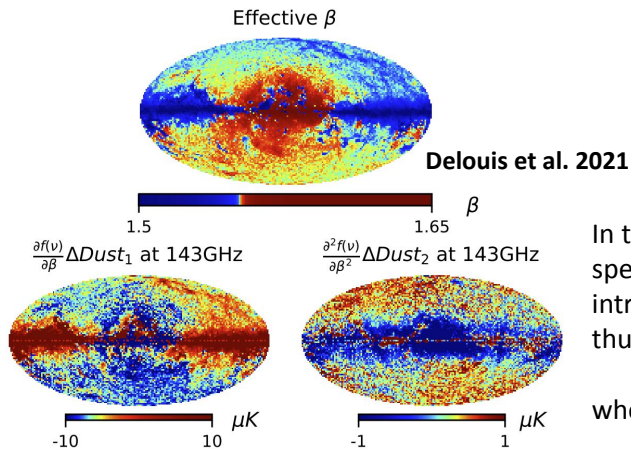
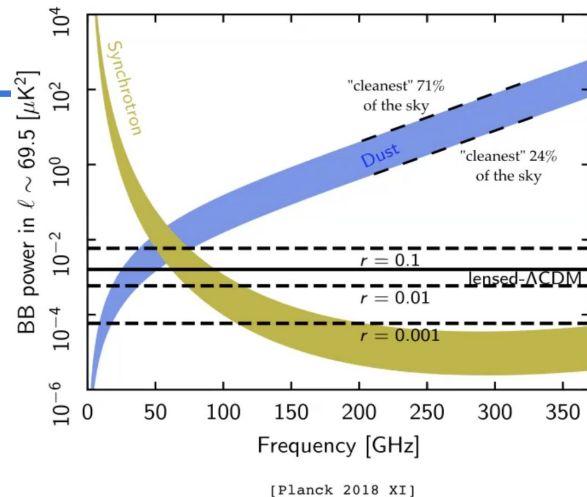
- **NIKA2Pol** high sensitive maps at **260 GHz** under investigation
- **SCUBA2Pol** at **353 GHz** proposal submitted



Foregrounds challenge

Main polarized foregrounds:

- Synchrotron emission
- Dust emission



In total intensity the large angular scale spatial variation of the dust spectral energy distribution (SED) is analytically described by introducing two additive SED corrections factors. The dust model is thus:

$$dust = f(\nu)Dust + \frac{\partial f(\nu)}{\partial \beta} \Delta Dust_1 + \frac{\partial^2 f(\nu)}{\partial \beta^2} \Delta Dust_2$$

where $f(\nu)$ is the Planck modified black-body function.

The correlation of these results with polarization data is under study (Ritacco+2021, in prep) and will be crucial to understand the behaviour of the dust polarization and prepare data analysis modelling for e.g. CMB-S4, LiteBIRD.

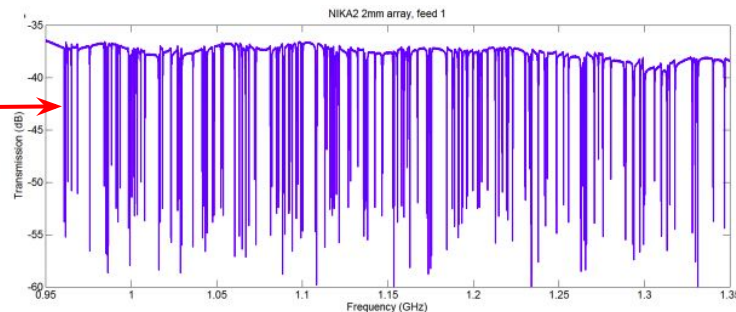
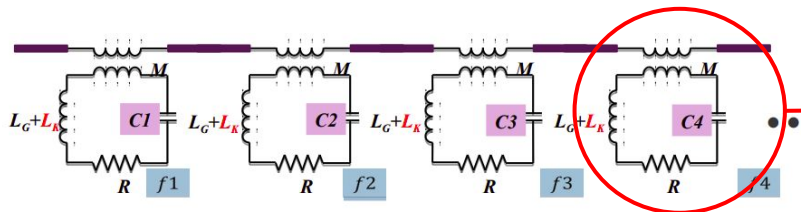
Summary

- ★ High control of the systematics induced by optical elements;
- ★ Modelling optical effects and propagating them into data analysis is the only way to choose the best configuration of polarization modulators;
- ★ Sky absolute calibration in a large frequency range is crucial for next generation of CMB experiments
 - current measurements could allow to probe $r = 10^{-2}$;
 - future accurate measurements of the Crab (e.g. NIKA2, SCUBA-2) are needed to meet the requirements of future CMB experiments to measure $r = 10^{-3}$ (e.g. LiteBIRD, CMB-S4).
- ★ Spatial dust SED variation has to be carefully accounted for in the component separation data modelling.

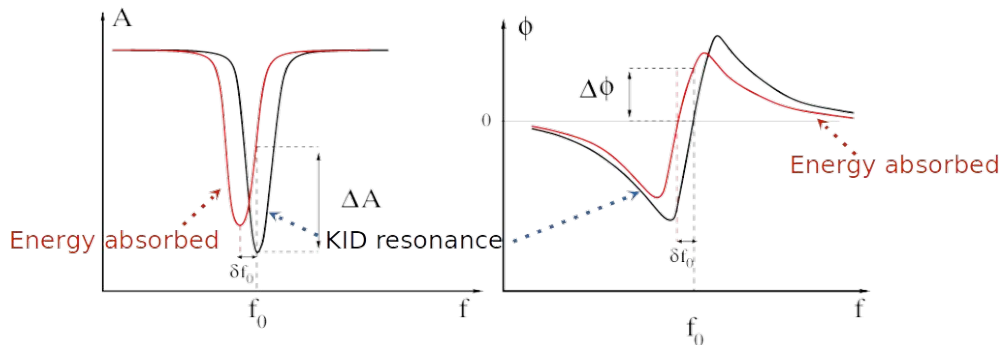
BACKUP SLIDES

Kinetic Inductance Detectors

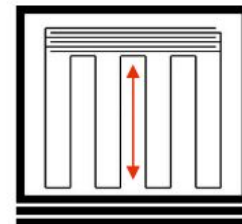
KIDs are RLC superconducting resonators



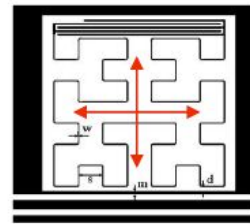
KIDs are intrinsically suited for Frequency Domain Multiplexing



$$\delta f_0 \propto -\delta P_{opt}$$



Sensitive to one polarization



Sensitive to both linear polarizations

Hilbert geometry

NIKA/NIKA2 detectors

NIKA2 KID array

- 2 mm array: 616 pixels \longrightarrow 4 feedlines
- 1.15 mm arrays: 1140 pixels \longrightarrow 8 feedlines

O. Bourrion et al.,
2012 JINST 7 P07014

